ObjectTrack: 6DoF Object Tracking Through UWB-IMU Fusion

Fan Jiang
Georgia Tech, Atlanta, USA
https://orcid.org/0000-0002-8636-6868

Frank Dellaert
Georgia Tech, Atlanta, USA
https://orcid.org/0000-0002-5532-3566

Ashutosh Dhekne
Georgia Tech, Atlanta, USA
https://orcid.org/0000-0001-6272-8521

***Abstract*—This paper presents a UWB-IMU fusion approach to obtain location and orientation of an object in 6 degrees of freedom at the room level, without use of optical motion capture systems. When tested with different human movement patterns such as walking, running, jumping, and swirling on a wheeled chair, we obtain less than 10cm of 3D localization error and under 5° of orientation error at the 90th percentile. We expect our system, called ObjectTrack, to enable spatial audio and interaction for VR/AR applications, enable precision tracking of objects, and for localization of robotic motion systems. ObjectTrack significantly reduces the cost barrier by about 50$\times$ compared to popular motion capture systems.**

***Index Terms*—UWB, 6DoF, UWB-IMU fusion, factor graphs**

I. Introduction and Related Work

Accurate real-time tracking of the six degrees of freedom (6DoF) pose (position and orientation) of objects within room level indoor environments is crucial for supporting augmented / virtual reality (AR/VR), tracking indoor robots, and human-computer interaction [1], [2]. Whereas optical motion capture (MoCap) systems provide high accuracy, they are quite expensive (at least $25K$ for an entry-level system). Further, optical systems suffer from line-of-sight requirements, sensitivity to lighting conditions, and high computational needs, restricting their use primarily to controlled lab environments.

This paper explores a way to combine Ultra-Wideband (UWB) radio ranging with Inertial Measurement Units (IMUs) to drastically reduce the cost of object tracking. Our goal is to achieve accurate and robust 6DoF object tracking in room-scale indoor spaces, overcoming several of the limitations of visual systems. UWB radios, operating under standards like IEEE 802.15.4z [12], use large bandwidths (> 500MHz) to achieve centimeter-level ranging precision and improved multipath resolution [10], while remaining robust to optical occlusions. However, UWB devices suffer from biases due to hardware and software delays, and standard protocols often lack the update rate and simultaneous ranging capabilities needed for smooth, high-fidelity tracking. Complementarily, IMUs provide high-frequency measurements of motion. Of course, naively integrating these measurements (dead-reckoning) yields high-frequency continuous pose estimates, but this process inherently suffers from drift accumulation over time due to sensor noise [18].

Fusing these complementary sensors presents significant challenges: synchronizing disparate data streams, mitigating UWB noise and multipath effects, correcting IMU drift and biases, and achieving real-time performance on resource-constrained platforms. We address these challenges with ObjectTrack, an end-to-end system designed for low-cost, high-performance 6DoF indoor object tracking.

Supported by NSF CAREER Grant #2145278 and Cisco Research.

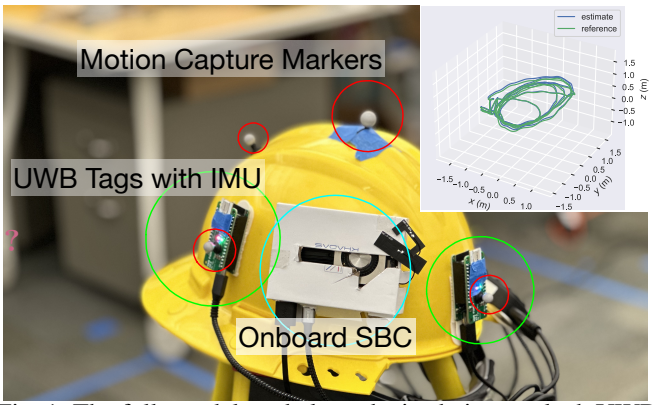

Fig. 1: The full standalone helmet device being tracked. UWB-IMU fusion is done on-board. Real-time pose information is downlinked to applications using Wi-Fi. Optical MoCap markers added for performance evaluation only.

Our key contributions are:

- A robust UWB-IMU fusion algorithm based on factor graphs [16] for real-time 6DoF pose estimation directly on an embedded platform attached to the tracked object.
- A novel cascaded UWB ranging protocol that significantly increases the ranging update rate and improves efficiency compared to standard two-way ranging.
- A comprehensive experimental evaluation of the ObjectTrack prototype in a $7\text{m} \times 9\text{m}$ room using 8 UWB anchors, demonstrating its performance against a professional OptiTrack MoCap system.

Our results show that ObjectTrack, built with components costing under $500, achieves a 90th percentile 6DoF tracking error of less than $10\,cm$ for **complex human trajectories**, demonstrating the feasibility of accurate, low-cost indoor object tracking using UWB-IMU fusion. An illustrative video is available at: https://tinyurl.com/objtrackvideo.

Several recent systems have also performed fusion of UWB and IMU data. Yao *et.al.*, in [20] have used extended kalman filters for predictable uniform motion. Zeng *et.al.* [22] and Feng *et.al.* in [6] have shown commendable results for a

robot moving on 2D surface. In the control literature, [9] have proposed a nonlinear complementary filter for localization of a drone without occulusion. In comparison, ObjectTrack works even for unpredictable human movements including jumping, running, and walking when occluded by another person.

In the learning literature, [17] have proposed a tight learned inertial-only odometry method. However, this method is highly dependent on the motion pattern of the tracked object. In comparison, ObjectTrack is able to track objects with arbitrary motion patterns.

II. System Overview

ObjectTrack enables real-time 6-DoF object tracking using a combination of UWB ranging and IMU measurements. Below we provide an overview of the calibration and deployment of the system, followed by a description of how the system functions during regular use. Deployment involves a technician installing a set of wireless anchors (typically 8) on the walls of the operational space, preferably at varying heights to improve 3D localization accuracy. These anchors are powered using AC mains power supply in our implementation, hence no power optimization is performed at the anchors. Anchor locations within the room's coordinate frame must be accurately determined through an assisted calibration procedure (Section III-C). The anchors do not require wired synchronization. The object to be tracked is instrumented with multiple tags, each equipped with an IMU. The relative location of UWB tags on the rigid object is measured and used for joint inferencing of the object's pose. These tags perform UWB ranging with the anchors and compute local sensor fusion using their IMUs. A one-time calibration step is necessary to estimate UWB range biases for each tag-anchor pair. This is achieved by moving the rigid body frame along a trajectory while collecting UWB range data, tracked either via self-calibration or an external system like MoCap for higher precision. This entire setup and calibration process is only one-time and typically requires only a few minutes.

During regular use, the always-on anchors continuously perform two-way ranging with nearby tags using our modified cascaded ranging protocol (Section III-A). Each tag collects range measurements from all visible anchors and combines this information with its own IMU data through a fusion algorithm. This fusion runs locally on the tag or a connected processing unit, generating real-time 6-DoF trajectory estimates. While the UWB update rate is determined by the ranging protocol and number of tags (it is 25 Hz for 3 tags in our implementation), the final tracking update rate leverages the high-frequency IMU data (up to 833 Hz), providing smooth and responsive tracking suitable for applications like virtual reality (Fig. 2). The system supports continuous operation with no inherent limit on how long the object can be tracked.

III. System Design

We now describe in detail, the algorithms developed for the regular use first, which are our primary contributions, and then discuss those for the one-time calibration.

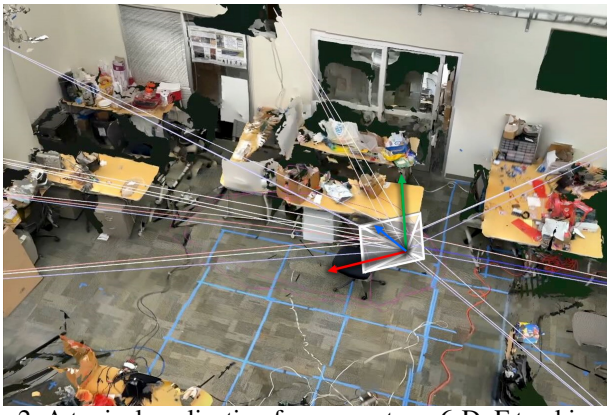

Fig. 2: A typical application for our system: 6-DoF tracking for virtual reality. Image captured from our real-time visualizer. Range rays indicate the error of range measurements. red/blue: shorter/longer, white: no error. Rays intersect at the 3 tag locations. Pyramid shows the user's current view frustum.

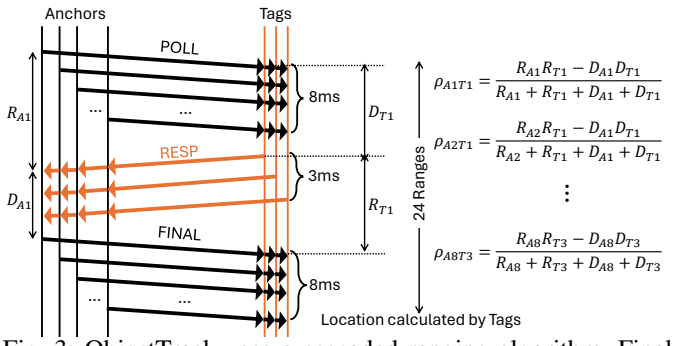

Fig. 3: ObjectTrack uses a cascaded ranging algorithm. Final location can be calculated by each individual tag.

A. Regular Use: Modified Cascaded Ranging Protocol

We have developed a modified ranging protocol to support fast multi-anchor ranging. Ranging between two UWB devices is defined in the IEEE 802.15.4z standard, comprising a POLL, RESP, and a FINAL message. Used naively for localization, range measurements between each anchor and tag will need to be sequential, consuming a significant amount of air-time. However, since UWB messages can be broadcast, it is possible to combine several of these sequential messages into a compressed sequence of message exchanges as shown in Fig. 3. Anchor Ax to tag Ty distance measurement is denoted as ρ_{AxTy} in the formulations shown in the figure. All anchors take turns in sending broadcast POLL messages which are received by three tags in this example. Each tag records the time at which each of the poll was received. After all polls have been received, each tag takes turns replying back with its own broadcast RESP message. The anchors record the received time for the RESP messages and then send this information back in the consecutive FINAL messages. Thus, each FINAL message contains its own transmit time and the receive timestamps of three RESP messages from the three tags. On receipt of the FINAL messages, the tags can calculate their distances from all 8 anchors, using the standard distance measurement formula shown in Fig. 3, meaning a total of 24

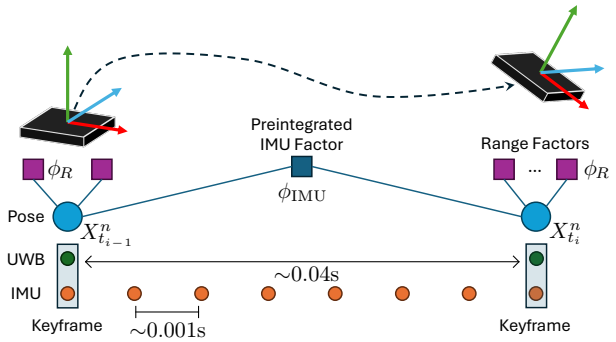

Fig. 4: UWB arrives at a much slower rate than IMU. Preintegration helps reducing the number of variables that we need to optimize. Note the IMU factor ϕ_{IMU} also connects to the bias variable, which we omitted here for brevity.

distance measurements are obtained by the 3 tags together. Robust 3D localization is then performed on the tags or at a compute node with which all the tags share their timestamp data, as described below.

B. Regular Use: Sensor Fusion for Object Tracking

We combine information obtained from inertial sensors with that obtained from UWB ranges to perform localization. Factor graphs are used in this process, and the reader is referred to the seminal work by Dellaert [4] on the topic.

1) Model for Wireless Ranging: The error characteristics (e.g. marginal distribution) of ranging errors differ significantly from scene to scene, among different indoor scenarios [3]. While more complex models, such as in [14], might be able to increase the localization accuracy, in this work we use a simple model for the ranging error, described below.

For each range measurement we define a (**unary**) factor, $\phi_R(P^n_{tag})$, which encodes the difference between the measured range z_R and the Euclidean distance $h_R(\cdot)$ between the estimated positions.

$$\phi_R(P^n_{tag}) = \|h_R(P^n_{tag}, P^n_{anchor}) + \beta_a + \beta_b - z_R\|_{\Sigma_R} \quad (1)$$

where P^n_{tag} is the tag's position, P^n_{anchor} is the anchor's position, β_a and β_b are the antenna biases of the tag and anchor, respectively, and Σ_R is the covariance matrix of the range measurement error.

2) IMU Preintegration:: We wish to integrate the faster IMU measurements ($833\,Hz$) with slower UWB range measurements ($\sim 25\,Hz$). However, direct IMU integration accumulates drift, and naive fusion incorporating every IMU sample is computationally expensive due to the significant rate mismatch (Fig. 4), requiring costly re-integration when correcting past states. To circumvent these issues, we perform IMU pre-integration between two UWB measurements. The object's state (rotation $\mathbf{R}_t$, velocity $\mathbf{V}_t$, position $\mathbf{P}_t$) evolves according to:

$$\begin{aligned} \tfrac{\mathrm{d}}{\mathrm{d}t}\mathbf{R}_t &= \mathbf{R}_t[\omega]_\times \\ \tfrac{\mathrm{d}}{\mathrm{d}t}\mathbf{V}_t &= \mathbf{g} + \mathbf{R}_t\mathbf{a}_t \\ \tfrac{\mathrm{d}}{\mathrm{d}t}\mathbf{P}_t &= \mathbf{V}_t \end{aligned} \quad (2)$$

where $\omega_t, \mathbf{a}_t$ are gyroscope and accelerometer readings.

To efficiently fuse these sensors, we use the IMU preintegration on manifold technique [7], summarizing IMU measurements between two UWB keyframes (t_i, t_j) into a single relative motion constraint, independent of the initial state. This constraint is represented by a factor ϕ_{IMU} on the NavState [7] manifold $X = \{R, P, V\}$:

$$\phi_{IMU}(X_i, X_j, b_i) = \|X_j \ominus \widehat{X_j}(X_i, b_i)\|_{\Sigma_{IMU}}, \quad (3)$$

where $\widehat{X_j}$ is the predicted state based on preintegrated measurements between X_i and X_j, and b_i is the IMU bias, estimated using a random walk model [5]. This factor enforces consistency between keyframes, leveraging faster IMU data to constrain motion and improve trajectory accuracy between sparse UWB updates.

3) Real-time Online Optimization: We are now able to define the factor graph of the complete problem. Since the calibration (tag-anchor range biases) is already known, the graph admits a very simple chain form, consisting of only **unary** range and **binary** IMU factors, which greatly improves performance. At keyframe t, we have

$$\begin{aligned} \Phi(X) = &\prod_{j\in A, k\in T, i} \phi_{R_{j,k,t_i}}(X^n_{t_i}) \cdot \prod_i \phi_{IMU}(X^n_{t_{i-1}}, X^n_{t_i}, b_{t_{i-1}}) \\ &\times \prod_i \phi_b(b_{t_{i-1}}, b_{t_i}) \end{aligned} \quad (4)$$

where $\phi_{R_{j,k,t_i}}$ is the range factor with known range biases and anchor location, ϕ_{IMU} the IMU factor described above, and ϕ_b the IMU bias random walk factor. The graph at t, $\Phi(X_t)$, is only a chain-like extension of $\Phi(X_{t-1})$, since the new factors depend only on the last and current state $X^n_{\{t-1,t\}}, b_{\{t-1,t\}}$.

This graph can be solved by an incremental smoother [16] with minimal complexity. This allows our system to operate in real-time with only a latency of $\sim 10\,ms$.

C. Calibration and Deployment

Calibration of ObjectTrack requires the precise determination of many unknown variables, such as the 3D location of anchors $\mathbf{p}_{A_n} \in \mathbb{R}^3$, the range biases for each antenna $\beta_k \in \mathbb{R}$, and the relative locations of each UWB tag on the object to be tracked (hard hat helmet in our case) $\mathbf{p}^b_{T_m}$. With N anchors and M tags, this gives us a total number of unknowns, D:

$$D = 3N + (N + M) + 3M \quad (5)$$

where we have an unobservable subspace of dimension $4 + 1$ which consists of the global translation, global yaw, and the arbitrary antenna bias zero point (as one could use any of the devices as zero antenna bias).

Optical systems are not immune from similar ambiguities (typically resolved using precisely measured calibration wands [8]). For initial calibration during installation, a technician moves the tracked object in a random manner around the capture volume. An external tracking source, such as a smartphone with ARKit or a high-precision motion capture system such as OptiTrack, provides ground truth trajectory information. The technician collects synchronized IMU and UWB ranging data while moving the tracked object within

the capture space. Simultaneously, we record the ground truth trajectory using the external tracking source.

We then use a factor graph to compute the maximum *a posteriori* (MAP) solution of all calibration variables, including anchor positions, device transforms, etc. We define here a quaternary range factor between each pair of devices (regardless of anchor or tag) for which a range measurement is available. The factor encodes the difference between the measured range z_R and the Euclidean distance $h_R(\cdot)$ between the estimated positions (note the difference with Equation (1)):

$$\phi_R(P_a^n, P_b^n, \beta_a, \beta_b) = \|h_R(P_a^n, P_b^n) + \beta_a + \beta_b - z_R\|_{\Sigma_R} \quad (6)$$

To handle potential non-line-of-sight measurements, we incorporate a robust cost function, here the Cauchy loss [21], into the range factors. These robust cost functions reduce the influence of outliers. The antenna biases for each tag (β_n^t) and anchor (β_m^a) are modeled as unknown parameters in the optimization problem. Similarly, the relative transformation between the body frame and the tag frame (P_{tag}^b) is estimated to determine the precise location of the tags on the tracked object. Mathematically, the graph is defined as

$$\Phi(X) = \prod_{i,j \in A \cup T, k} \phi_{R_{t_k}}(\cdots) \cdot \prod_i \phi_{IMU}(X_{t_{i-1}}^n, X_{t_i}^n, b_{t_{i-1}}) \times \prod_i \phi_b(b_{t_{i-1}}, b_{t_i}) \times \prod_{i \in A, k} \phi_P(P_{i,t_k}^n) \times \prod_i \phi_X(X_t^n) \quad (7)$$

where A set of anchors, T the set of tags, $\phi_{R_{t_k}}$ are the range factors at keyframe time t_k, ϕ_{IMU} the IMU factor, ϕ_b the IMU bias random walk factor, and ϕ_P and ϕ_X are the prior factors for the anchor positions and body trajectory.

IV. Implementation

A. Hardware Design

Accurate motion and orientation tracking with UWB and IMU requires two features: (i) accurate synchronization of UWB measurements with IMU data, which is paramount to correct data association during the fusion process, and (ii) high quality IMU measurements with relatively stable IMU bias. To achieve this, we used our custom hardware platform [15], and custom software library based on Rust, that integrates UWB and IMU measurements with microsecond-level timestamps.

The same hardware is used both as a tag and as an anchor. An ESP32-S3 microprocessor serves as the main processing unit. An LSM6DSO IMU is used to deliver inertial measurements at 833Hz. To enable standalone operation, the platform also includes a SGM41511 battery management system (BMS) that supports LiPo battery. A DWM3000 [19] is used as the UWB radio. The entire package is miniaturized to a small $5\,cm \times 2\,cm \times 1.5\,cm$ block (see a photo in Fig. 6), so that it can be easily attached to any moving object that needs to be tracked. The onboard computer is a Khadas VIM4 single-board computer that connects to the UWB tags via USB.

B. Software Design

To ensure seamless deployment and operation of ObjectTrack in real-world scenarios, we have designed a robust and fault-tolerant Rust-based software architecture that prioritizes ease of configuration, safety, and modularity. The software design is centered around the ZeroMQ [11] messaging library, which provides a high-performance message queue and a publisher/subscriber communication model. As far as we know, this is the first ever UWB and IMU object tracking platform using the Rust programming language.

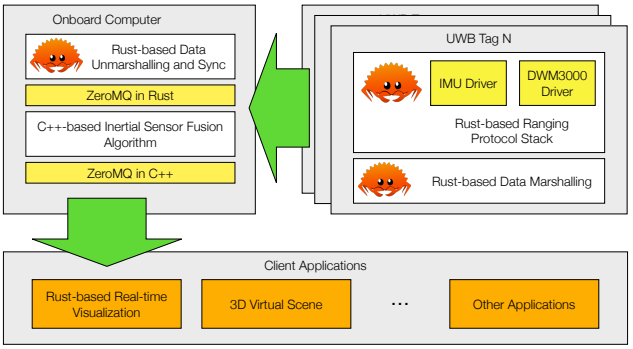

Fig. 5: Rust-based software pipeline system diagram.

Figure 5 illustrates the overall software system diagram. All system information, including sensor data and fusion results, is transmitted as ZeroMQ message topics. This approach enables any client application to subscribe to the relevant topics, facilitating easy integration and abstraction of the client applications from the internal workings of the system.

The software components running on the UWB tags and the onboard computer are implemented using the Rust programming language, reducing the risk of common programming errors and enabling optimal utilization of system resources.

V. Evaluation

In order to evaluate the accuracy and robustness of our proposed system, we set up our system in a few typical use cases and challenging scenarios. All experiments are conducted inside our lab with an OptiTrack motion capture system serving as ground truth, which typically has ∼0.1mm accuracy when all markers on the rigid body are tracked.

Our evaluation environment is shown in Fig. 6. The ground truth anchor locations are obtained with a Leica TCR703 Total station (∼$2500) with an accuracy of ∼3mm (anchors are outside the OptiTrack tracked volume). Anchors are then co-located within the motion capture frame by measuring fixed markers placed inside the motion capture tracking volume (about $4\,m \times 4\,m$), which is smaller than ObjectTrack's total capture volume. The marker location on the tracked rigid body is identified automatically by our calibration system.

We run all real-time experiments on the onboard computer with an Amlogic A311D2 ARM processor. All metrics, visualization and other data processing are done on a ThinkPad X1 Yoga Gen 8 Laptop with Intel Core i7-1365U processor.

A. Object Localization Accuracy

We evaluate ObjectTrack's localization and orientation accuracy against OptiTrack ground truth using precisely calibrated anchor locations and best-case biases. A researcher performed six diverse actions (walking near/with another

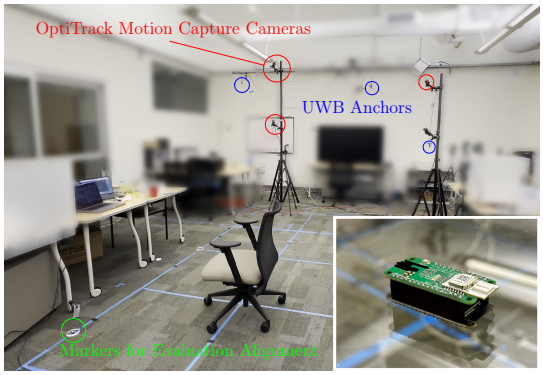

Fig. 6: ObjectTrack evaluation setup in our lab.

person creating partial occlusions, walking/jumping, hopping, running, and spinning on a chair). Raw data and trajectories will be open-sourced creating a first of its kind dataset. These movements were captured by UWB, IMU, and OptiTrack (Fig. 1). We first assess the full system (ObjectTrack) using UWB and IMU fusion, then perform ablation studies. Periods of limited OptiTrack confidence due to marker occlusion are marked by red intervals on timeline graphs.

1) ObjectTrack with 3 UWB tags, IMU, and data post-processing: Fig. 7a shows the best-estimate Absolute Position Error (APE) CDF using three UWB tags, IMU, and rigid body constraints. The 90^{th} percentile accuracy is under $10\,cm$ for most activities. The 3D trajectories (Fig. 8) and APE timeline (Fig. 9, black trace) demonstrate robust localization with minimal deviation from ground truth. Fig. 10 shows rotation error. Apparent large rotation errors during OptiTrack occlusion periods (red intervals) are artifacts of the ground truth system's sensitivity to marker occlusion, unlike the more robust IMU/UWB fusion in ObjectTrack.

2) Real-time Trajectory Estimation: Without access to future data, real-time estimation (Fig. 7b) achieves a 90^{th} percentile APE between $12-17\,cm$. Real-time position and rotation errors are overlaid in blue on Figures 9 and 10.

3) Ablation Study: With only 3 UWB Tags (no IMU): Removing the IMU significantly degrades performance. Using only three UWB tags yields a 90^{th} percentile APE between $20-30\,cm$ (Fig. 7c). While median error remains below $15\,cm$ and trajectories are decipherable (Fig. 11), worst-case errors increase and poses become discontinuous.

4) Ablation Study: With 1 UWB Tag and IMU: Using only one UWB tag with the IMU increases the 90^{th} percentile APE slightly ($\sim$1 cm) compared to three tags (Fig. 12), demonstrating the complementary nature of UWB and IMU. Initialization takes longer as initial pose and biases must be estimated, but accuracy quickly converges.

B. Robustness: Challenging Scenarios

ObjectTrack maintains robust and accurate tracking ($<10\,cm$ 90^{th} percentile APE, $<5^{\circ}$ rotation error) across challenging scenarios designed to induce occlusion, dynamic multi-path, and high-speed motion (Fig. 8). These include movement near/with another person, jumping, running ($\sim$5m/s), and spinning while seated on a chair.

C. System Considerations

1) Power Consumption: Our tags consume about $450\,mW$ of power on an average with their UWB and IMU turned on continuously, powered by an ESP32 microcontroller, with no power optimizations. In comparison, a 50% duty cycling mmWave radar [13] would consume about $2.14\,W$.

2) UWB Update Rate: ObjectTrack obtains a reliable UWB 3-tag localization update rate of $25\,Hz$ due to our modified cascaded ranging protocol (see Fig. 13). Without our optimizations in the ranging protocol, the best possible update rate would have been only $\sim 8\,Hz$.

VI. Conclusion

ObjectTrack is an exploration in closing the gaps in UWB-IMU based 3D object tracking. We have developed a method to fuse information from IMU and UWB sensors which benefits each other in improving tracking speed and limiting drift over time. We expect that by lowering the costs associated with object tracking, we might lower the barrier to entry and bring this technology, though slightly inaccurate, to a larger audience. We fully expect the research community to build upon the foundations laid in this paper, improving upon the limitations of ObjectTrack, for years to come.

References

[1] Aditya Arun, Shunsuke Saruwatari, Sureel Shah, and Dinesh Bharadia. XRLoc: Accurate UWB Localization to Realize XR Deployments, November 2023.

[2] Tara Boroushaki, Isaac Perper, Mergen Nachin, Alberto Rodriguez, and Fadel Adib. Rfusion: Robotic grasping via rf-visual sensing and learning. In *Proceedings of the 19th ACM conference on embedded networked sensor systems*, pages 192–205, 2021.

[3] Haige Chen and Ashutosh Dhekne. Pnploc: Uwb based plug & play indoor localization. In *2022 IEEE 12th International Conference on Indoor Positioning and Indoor Navigation (IPIN)*. IEEE, 2022.

[4] Frank Dellaert. Factor graphs and gtsam: A hands-on introduction. *Georgia Institute of Technology, Tech. Rep*, 2(4), 2012.

[5] Jay A. Farrell, Felipe O. Silva, Farzana Rahman, and Jan Wendel. Inertial measurement unit error modeling tutorial: Inertial navigation system state estimation with real-time sensor calibration. *IEEE Control Systems Magazine*, 42(6):40–66, 2022.

[6] Daquan Feng, Chunqi Wang, Chunlong He, Yuan Zhuang, and Xiang-Gen Xia. Kalman-filter-based integration of imu and uwb for high-accuracy indoor positioning and navigation. *IEEE Internet of Things Journal*, 7(4):3133–3146, 2020.

[7] Christian Forster, Luca Carlone, Frank Dellaert, and Davide Scaramuzza. On-Manifold Preintegration for Real-Time Visual–Inertial Odometry. *IEEE Transactions on Robotics*, 33(1):1–21, February 2017.

[8] Joshua S Furtado, Hugh H T Liu, Gilbert Lai, Herve Lacheray, and Jason Desouza-Coelho. Comparative Analysis of OptiTrack Motion Capture Systems. In *Advances in Motion Sensing and Control for Robotic Applications: Selected Papers from the Symposium on Mechatronics, Robotics, and Control (SMRC'18)-CSME International Congress 2018, May 27-30, 2018 Toronto, Canada*, pages 15–31. Springer, 2019.

[9] Hashim A. Hashim, Abdelrahman E. E. Eltoukhy, and Kyriakos G. Vamvoudakis. Uwb ranging and imu data fusion: Overview and nonlinear stochastic filter for inertial navigation. *Trans. Intell. Transport. Sys.*, 25(1):359–369, January 2024.

[10] Alexander Heinrich, Sören Krollmann, Florentin Putz, and Matthias Hollick. Smartphones with UWB: Evaluating the Accuracy and Reliability of UWB Ranging, March 2023. arXiv:2303.11220 [cs].

[11] Pieter Hintjens. *ZeroMQ: Messaging for Many Applications*. O'Reilly Media, 2013.

[12] IEEE. Ieee standard for low-rate wireless networks–amendment 1: Enhanced ultra wideband (uwb) physical layers (phys) and associated ranging techniques. *IEEE Std 802.15.4z-2020 (Amendment to IEEE Std 802.15.4-2020)*, pages 1–174, 2020.

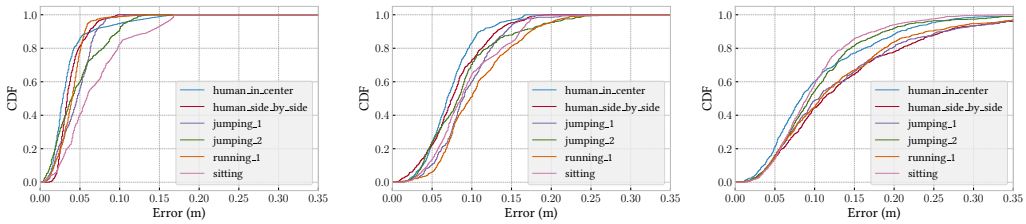

(a) Using 3 UWB tags and IMU (Post-processing). (b) Realtime: Using 3 tags and IMU. (c) Using 3 UWB tags without IMU.

Fig. 7: CDFs of 3D Position Errors: various UWB/IMU configurations. (Full, 1×UWB+IMU, 3×UWB Only, Self Calibration)

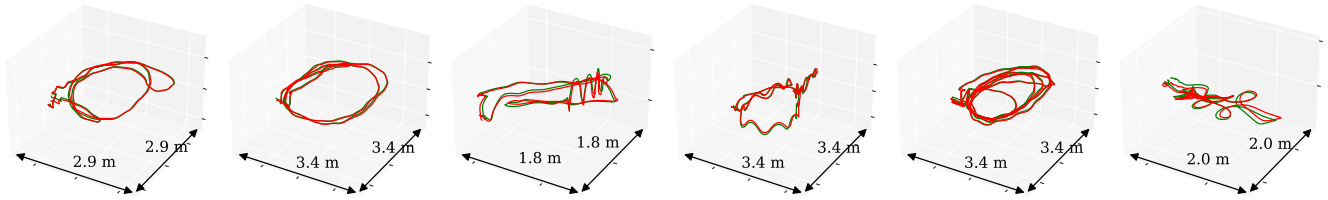

(a) human in center (b) human side by side (c) jumping 1 (d) jumping 2 (e) running 1 (f) sitting

Fig. 8: 3D trajectory after post-processing. Green using 3 tags and IMU. Red: Reference Ground Truth (zoom-in to see details)

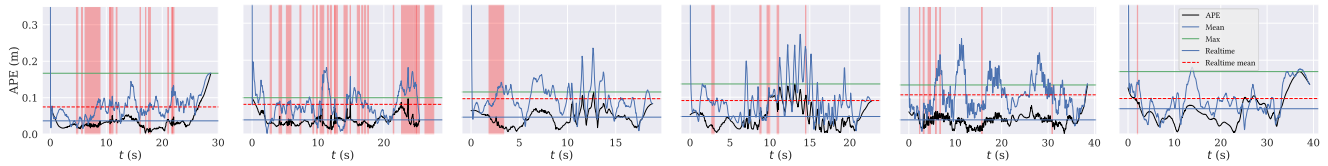

(a) human in center (b) human side by side (c) jumping 1 (d) jumping 2 (e) running 1 (f) sitting

Fig. 9: Timeline: APE using 3 tags and IMU. OptiTrack low confidence times are indicated in red.

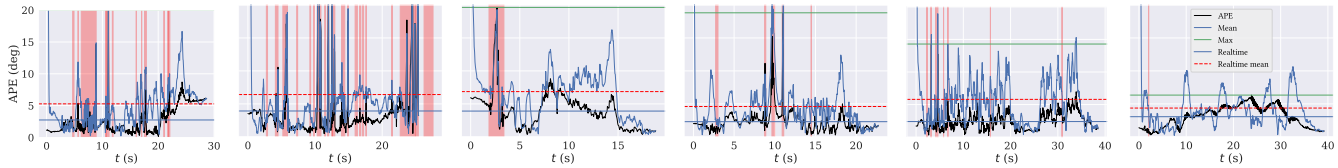

(a) human in center (b) human side by side (c) jumping 1 (d) jumping 2 (e) running 1 (f) sitting

Fig. 10: Timeline: Absolute Rotation Error in degrees using 3 tags and IMU.

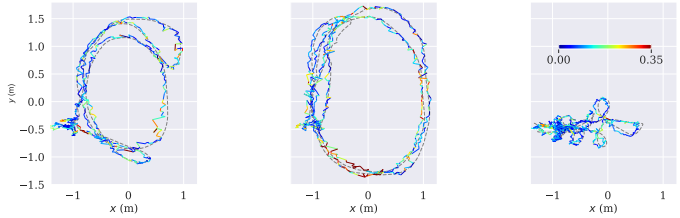

(a) human in center (b) human side by side (c) sitting

Fig. 11: Abalation: 3D trajectory (X-Y) using 3 tags UWB, wi

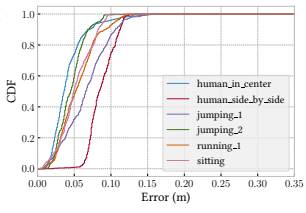

Fig. 12: Best-estimate APE 1 UWB with IMU.

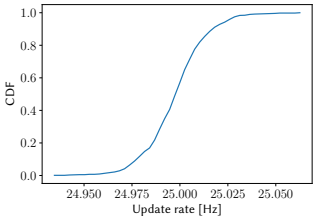

Fig. 13: Observed UWB update rate.

[13] Texas Instruments. Awr1642 single-chip 76-ghz to 81-ghz automotive radar sensor evaluation module, 2024.

[14] Fan Jiang, David Caruso, Ashutosh Dhekne, Qi Qu, Jakob Julian Engel, and Jing Dong. Robust indoor localization with ranging-imu fusion, 2024.

[15] Fan Jiang and Ashutosh Dhekne. Demo: uFiμ: An open-source integrated UWB-WiFi-IMU platform for localization research and beyond. In *Proceedings of the 25th International Workshop on Mobile Computing Systems and Applications*, pages 156–156, San Diego CA USA, February 2024. ACM.

[16] Michael Kaess, Hordur Johannsson, Richard Roberts, Viorela Ila, John J Leonard, and Frank Dellaert. iSAM2: Incremental smoothing and mapping using the Bayes tree. *The International Journal of Robotics Research*, 31(2):216–235, February 2012.

[17] Wenxin Liu, David Caruso, Eddy Ilg, Jing Dong, Anastasios I. Mourikis, Kostas Daniilidis, Vijay Kumar, and Jakob Engel. Tlio: Tight learned inertial odometry. *IEEE Robotics and Automation Letters*, 5(4):5653–5660, 2020.

[18] T. Lupton and S. Sukkarieh. Visual-Inertial-Aided Navigation for High-Dynamic Motion in Built Environments Without Initial Conditions. *IEEE Trans. Robotics*, 28(1):61–76, February 2012.

[19] Qorvo. Dwm3000, 2024.

[20] Leehter Yao, Yeong-Wei Andy Wu, Lei Yao, and Zhe Zheng Liao. An integrated imu and uwb sensor based indoor positioning system. In *2017 International Conference on Indoor Positioning and Indoor Navigation (IPIN)*, pages 1–8, 2017.

[21] Zhengyou Zhang. Parameter estimation techniques: a tutorial with application to conic fitting. *Image and Vision Computing*, January 1997.

[22] Shuaikang Zheng, Zhitian Li, Yunfei Liu, Haifeng Zhang, and Xudong Zou. An optimization-based uwb-imu fusion framework for ugv. *IEEE Sensors Journal*, 22(5):4369–4377, 2022.